Article

Synchronization of Midbrain Dopaminergic Neurons Is Enhanced by Rewarding Events

Mati Joshua,[1,2,*] Avital Adler,[1,2] Yifat Prut,[1,2] Eilon Vaadia,[1,2] Jeffery R. Wickens,[4] and Hagai Bergman[1,2,3]
[1]Department of Physiology, The Hebrew University-Hadassah Medical School, Jerusalem 91120, Israel
[2]The Interdisciplinary Center for Neural Computation
[3]Eric Roland Center for Neurodegenerative Diseases
The Hebrew University, Jerusalem 91904, Israel
[4]Okinawa Institute of Science and Technology, 12-22, Suzaki, Uruma, Okinawa 904-2234, Japan
*Correspondence: mati@alice.nc.huji.ac.il

SUMMARY

The basal ganglia network is divided into two functionally related subsystems: the neuromodulators and the main axis. It is assumed that neuromodulators adjust cortico-striatal coupling. This adjustment might depend on the response properties and temporal interactions between neuromodulators. We studied functional interactions between simultaneously recorded pairs of neurons in the basal ganglia while monkeys performed a classical conditioning task that included rewarding, neutral, and aversive events. Neurons that belong to a single neuromodulator group exhibited similar average responses, whereas main axis neurons responded in a highly diverse manner. Dopaminergic neuromodulators transiently increased trial-to-trial (noise) correlation following rewarding but not aversive events, whereas cholinergic neurons of the striatum decreased their trial-to-trial correlation. These changes in functional connectivity occurred at different epochs of the trial. Thus, the coding scheme of neuromodulators (but not main axis neurons) can be viewed as a single-dimensional code that is further enriched by dynamic neuronal interactions.

INTRODUCTION

Technical advances enabling recordings of the simultaneous activity of several neurons (Abeles, 1982; Eggermont, 1990; Baker et al., 1999) have made it possible to study the properties of neuronal networks. Early studies (Perkel et al., 1967; Abeles, 1982; Aertsen et al., 1989; Bartho et al., 2004) focused on detection and quantization of the functional connectivity between neurons (e.g., direct excitatory, inhibitory synapses or common synaptic inputs). In the basal ganglia (Bergman et al., 1998), this approach was used to provide insights into the debate regarding the existence of parallel segregated basal ganglia pathways (Alexander et al., 1986) versus a convergent funneling architecture (Percheron et al., 1984; Percheron and Filion, 1991). Recent studies have used data from simultaneously recorded

neurons to examine issues related to encoding/decoding and information processing in the nervous system (Gawne and Richmond, 1993; Schneidman et al., 2003; Averbeck et al., 2006). One study conducted by our group (Nevet et al., 2007) showed that contrary to the positive noise and signal correlation found between pairs of cortical neurons (Gawne and Richmond, 1993; Zohary et al., 1994; Lee et al., 1998; Yanai et al., 2007), the average correlation in the substantia nigra pars reticulata (SNr) population does not differ significantly from zero. However, there are no studies of correlations exploring the similarity of average responses of neurons in other structures of the basal ganglia such as the globus pallidus external and internal segments (GPe and GPi respectively) on the one hand, or the neuromodulators of the basal ganglia, such as tonically active neurons (TANs, striatal cholinergic interneurons) and midbrain dopaminergic neurons (DANs) on the other. Moreover, there are no studies on the basal ganglia that have examined dynamics in the correlation of trial-by-trial discharge variations; i.e., the dynamics of the noise correlation.

The division of the basal ganglia into neuromodulator and main axis subsystems is based on both anatomical (Parent and Hazrati, 1995; Haber and Gdowski, 2004) and physiological properties of these neurons (DeLong, 1971; Grace and Bunney, 1983a; Kimura et al., 1984; Joshua et al., 2008, 2009). It was suggested that the neuromodulators provide the network a single-dimensional signal (scalar) and that the main axis utilizes this scalar (Schultz, 1998; Bar-Gad et al., 2003). The most common basal ganglia models suggest that they operate as a reinforcement learning system in which the DANs encode the temporal-difference prediction error (Schultz et al., 1997). These models assume that the teaching message is transmitted to all striatal territories, and the neural plasticity of the cortico-striatal synapses is regulated by a homogenous dopamine signal and selective cortico-striatal activity (Arbuthnott and Wickens, 2007). The cholinergic interneurons are assumed to mediate or complement the teaching message of the DANs (Centonze et al., 2003; Pisani et al., 2007). Models that include the basal ganglia main axis suggest that by contrast to the scalar nature of the neuromodulators, the main axis activity is diverse (Mink, 1996; Bar-Gad et al., 2003). The GABAergic lateral connections in the main axis (Tunstall et al., 2002; Plenz, 2003; Haber and Gdowski, 2004) support the notion of a competitive component in the activity of main axis neurons (Fukai and Tanaka, 1997; Frank et al., 2004).
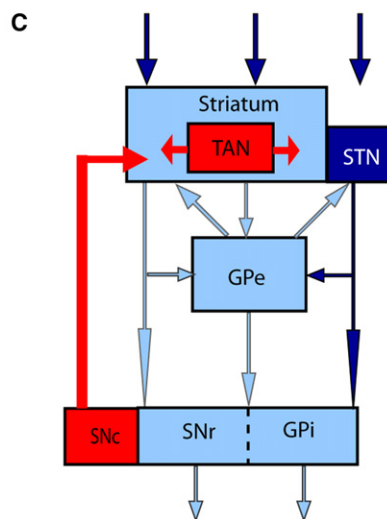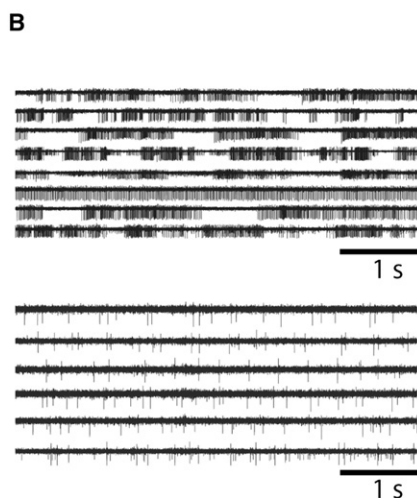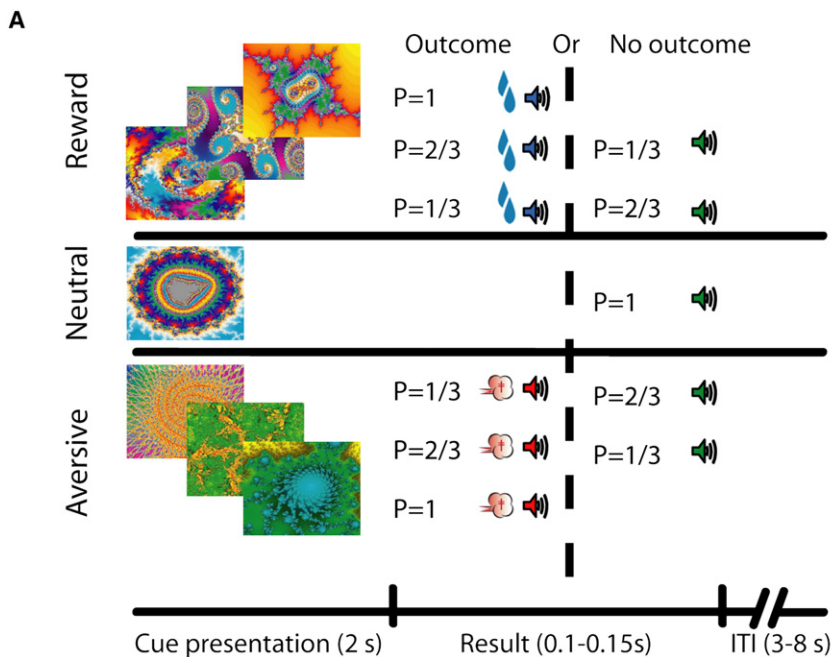
Figure 1. Recording and Behavioral Task

(A) Behavioral task. Classical conditioning task with three cues that predicted a food outcome (reward cues), three cues predicted an airpuff outcome (aversive cues), and one neutral cue. The outcome delivery on each trial was randomized according to a fixed probability associated with the trial cue. Cues were randomized between monkeys and are shown as presented to monkey S.

(B) Top: Simultaneous extracellular recordings from eight electrodes in the globus pallidus. In seven electrodes the cells were classified as GPe pausers, and one of the cells was classified as a pallidal border cell (electrode 6). Bottom: Simultaneous extracellular recordings of TANs from six electrodes in the striatum. Data are shown after 300–6000 Hz digital band-pass filtering.

(C) A schematic diagram of basal ganglia connectivity. Dark blue arrows indicate glutamatergic excitatory connections; light blue arrows, GABAergic inhibitory connections; red, neuromodulators. Abbreviations: GPe indicates external segment of the globus pallidus; GPi, internal segment of the globus pallidus; SNc, substantia nigra pars compacta; SNr, substantia nigra pars reticulata; STN, subthalamic nucleus; TAN, tonically active neurons (putative striatal cholinergic interneurons).

The recent development of efficient tools for simultaneous recording of multineuron activity from the basal ganglia makes it possible to explore the correlation of basal ganglia neurons. Given the above, our working hypothesis predicts that the responses of neuromodulators should be homogenous and synchronized whereas main axis activity should be diverse and independent. In addition, the temporal modulation of noise correlation (Aertsen et al., 1989; Vaadia et al., 1995; Baker et al., 2001) might provide another domain, beyond rate and pattern, for neuronal encoding.

Three cues predicted a food outcome (reward cues) with a delivery probability of 1/3, 2/3, and 1, and three cues predicted an airpuff outcome (aversive cues) with a delivery probability of 1/3, 2/3, and 1. The seventh cue (the neutral cue) was never followed by a food or an airpuff outcome. Thus the task contained 18 different events, i.e., 7 different cues and 11 cue-outcome/no-outcome combinations. During the task we recorded the spiking activity of two to eight electrodes simultaneously (see Figure 1B for an example of simultaneous recordings of eight electrodes in the globus pallidus and for the simultaneous recording of six electrodes in the striatum that show activity of TANs). To avoid bias caused by shadowing effects (Lewicki, 1998; Bar-Gad et al., 2001), we limited this study to units recorded by different electrodes. Our neural database included 163 TANs, 144 DANs, 368 GPe, 158 GPi, and 174 SNr pairs of neurons (see Figure 1C for schematic network diagram) that were recorded simultaneously and satisfied the study inclusion criteria (see Experimental Procedures) for more than 30 successive minutes during task performance.
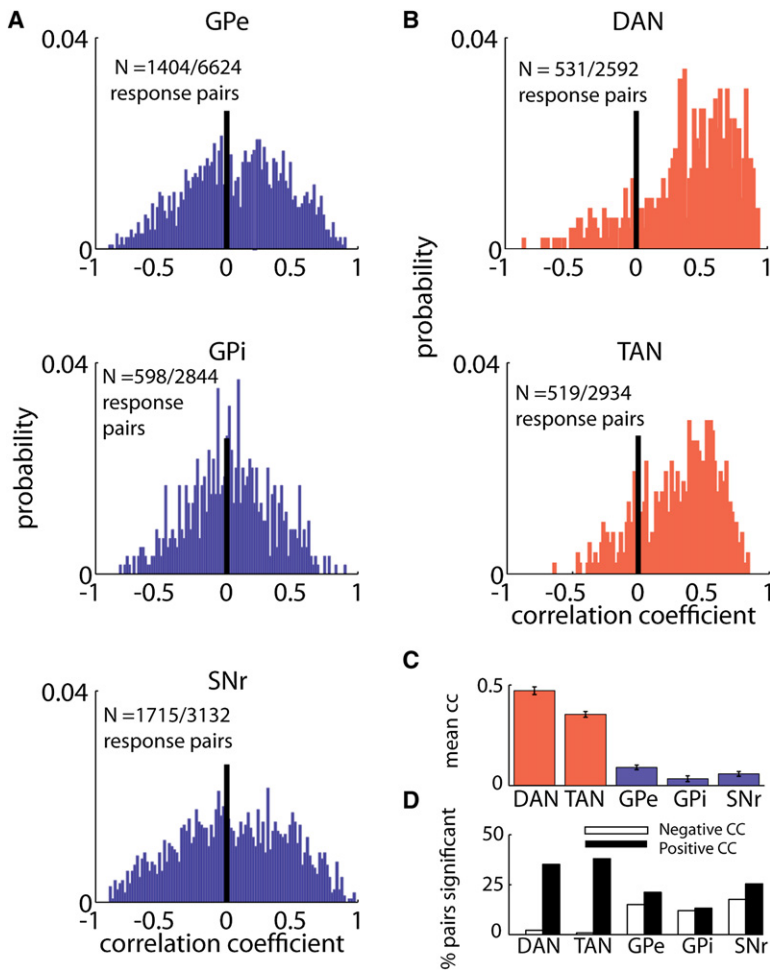
RESULTS

Behavior Task and the Neuronal Data Base

Two monkeys were introduced to seven different visual cues, each predicting the outcome in a probabilistic manner (Figure 1A).

Response Homogeneity of Neuromodulators versus Diversity of Responses in the Main Axis of Basal Ganglia Networks

We used the response correlation (Nevet et al., 2007) to quantify the similarity of the responses of a pair of cells to the same event.

Figure 2. Response Correlation Reveals Similarity of Responses of the Basal Ganglia Modulators versus Heterogeneity of Responses of Main Axis Neurons

(A) Distribution of the GPe, GPi, and SNr (main axis) response correlations. Only responses with significant rate modulations of both neurons were included. N indicates number of included response pairs out of the total number of response pairs. For this analysis we constructed the PSTHs for the 2 s after the event onset in bins of 1 ms and smoothed them with a Gaussian filter of SD = 20 ms.

(B) Distribution of the DAN and TAN (neuromodulators) response correlations (same conventions as in A).

(C) The mean and SEM of the response correlation in each of the recorded populations.

(D) The percentage of significant response correlations (t test; $p < 0.05$). Black indicates positive response correlations; white, negative response correlations. The smoothing of the PSTHs leads to dependency between bins, and hence for the significance testing we constructed the PSTHs in bins of 50 ms with no smoothing.

Response correlation analysis tests the correlation between pairs of responses to single events; however, it does not directly test the correlation between the average responses of pairs of neurons to more than one event. To test whether encoding of different events is correlated we performed signal correlation analysis (Gawne and Richmond, 1993; Lee et al., 1998; Averbeck and Lee, 2004). We found that the signal and response correlation analysis yielded similar results; i.e., the distribution of the signal correlation of the neuromodulators was skewed toward positive values and for the main axis the signal correlation was symmetrically distributed with an average close to zero (see Figures S1A–S1D available online). Comparing the signal and response correlations showed that these two correlation measures were correlated (Figure S1E). This indicates that the cell pairs with comparable temporal response pattern are those that encode different events similarly. To summarize, the average responses of the basal ganglia neuromodulators (TANs and DANs) were homogeneous, in contrast to the diverse responses of neurons in the main axis of the basal ganglia (GPe, GPi, and SNr).

Reward Expectation and Delivery Enhances Temporal Modulation of DAN Correlations

The response and signal correlations are measures of the correlation of the average responses (across trials) of two cells and do not take into account the dynamic changes in their noise correlation (correlations between variations from the average response) that can occur within a given epoch (see Figure S2 for average noise correlation). We therefore calculated the joint peristimulus histogram (JPSTH) (Gerstein and Perkel, 1969; Aertsen et al., 1989; Vaadia et al., 1995). The JPSTH is obtained by subtracting the PSTH predictors from the raw coincident count matrix to obtain an estimate of the unpredicted correlations, i.e., correlations beyond those predicted by the modulation of

The response correlation is the correlation coefficient between two average responses (poststimulus time histogram [PSTH]) and hence quantifies the similarity of the temporal pattern of the responses. Figure 2 shows the distribution of the response correlation analysis for all studied populations. The response correlations for the GPe, GPi, and SNr neurons were symmetrically distributed with an average close to zero (Figure 2A). However, the distribution of the response correlation of DANs and TANs was skewed toward positive values (Figure 2B). The mean response correlation of the neuromodulators was larger than the mean correlation for the main axis ($p < 0.001$; t test on the z transformed values, Figure 2C). We found that the difference was also apparent in the fraction of significant positive and negative response correlations. A large proportion of the positive response correlations of the DANs and TANs were significantly different from zero, but this was true for only a small proportion of the negative correlations (Figure 2D). In the GPe, GPi, and SNr, although many of the response correlations were significantly different from zero, the proportion of cells with positive and negative response correlations was similar (Figure 2D). We conclude that the neuromodulators of the basal ganglia have homogenous responses whereas the responses of the main axis are diverse.
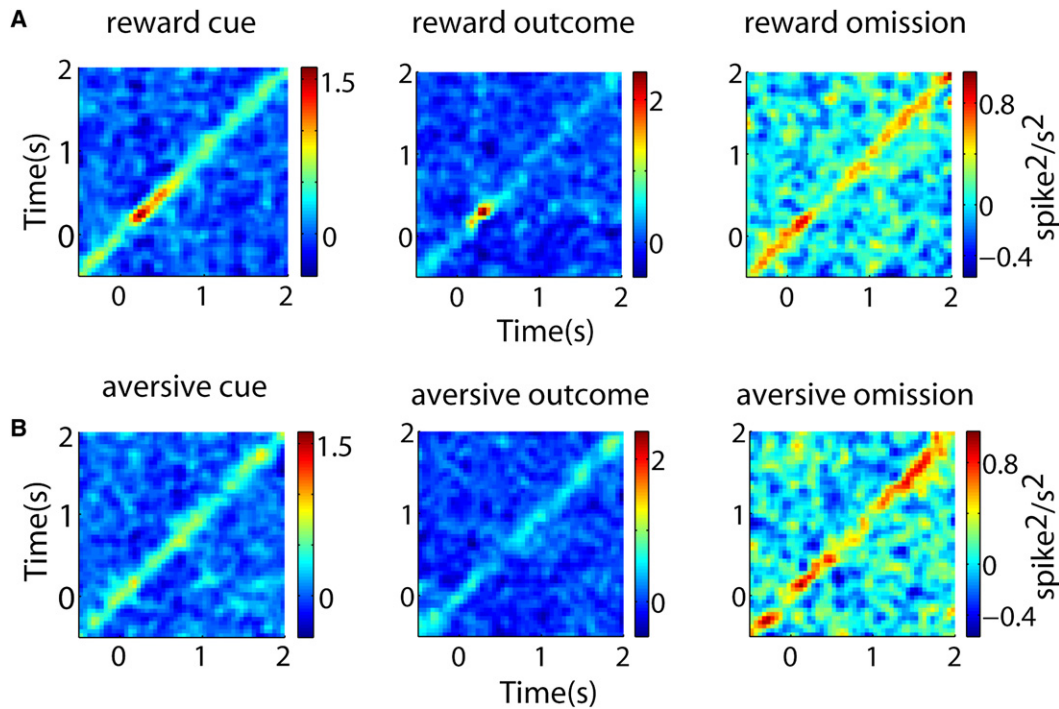
Figure 3. Noise Correlation of DAN Pairs Increased with Expectation of Reward and Reward Delivery but Not for Aversive Events
(A) The population JPSTH of the DANs (n = 144 pairs) for the reward trials. Left, cue; middle, outcome; right, no outcome. Bin size 50 × 50 ms, smoothed with a two-dimensional Gaussian filter with SD = 1 bin. The different JPSTHs have different intensity (color bars on the right) scales to enhance the visibility of the correlation dynamics.
(B) The DAN population JPSTH for aversive trials. Corresponding epochs in (A) and (B) have the same color scaling to enable comparison of aversive and reward JPSTHs.

the average discharge rate (see Figure S3 for three examples of JPSTH analysis). Note that the JPSTH diagonal quantifies the time-dependent modulation of zero lag noise correlation.

We extended the JPSTH analysis of a single neuron pair to the populations of neuromodulator neurons. To examine whether the DANs noise correlation depends on the context of the behavioral task, we analyzed the reward and aversive trials separately. In Figure 3 we show the separation of the DAN population JPSTHs into reward and aversive trials. In the cue and outcome epochs, the DAN noise correlation increased only for the reward trials (Figure 3A) but not for the aversive trials (Figure 3B). Testing for differences between the average JPSTH diagonal before and after the event (paired t test on the average diagonal comparing −0.5–0.0 s versus 0.1–0.6 s) shows that there was a substantial increase in the noise correlation for the reward cue (p < 0.01) and outcome (p < 0.001) as compared with a nonsignificant increase for the aversive cue (p = 0.46) and a nonsignificant decrease for the aversive outcome (p = 0.06).

The JPSTH analysis revealed changes in the synchronization level beyond those expected by the changes in firing rate (Aertsen et al., 1989). In Figure 4 we show the comparison between synchronization and rate modulations (JPSTH and predictor diagonals, respectively). We found that although there was an increase in rate for both reward and aversive trials (Figure 4A and Joshua et al., 2008), the increase in the noise correlation was found only in the reward trials (Figure 4B, and see Figure 4C

for a comparison of noise correlation dynamics for epochs with similar rate modulation). Furthermore, the JPSTH analysis for the subset of dopaminergic pairs that simultaneously increase their firing rate to aversive outcome shows that the noise correlation of these cells does not increase (Figure S4).

JPSTH analysis of the TANs did not reveal a correlation encoding of the rewarding versus aversive events (Figure S5). Figure 5 shows the results of the significance test (paired t test) comparing the JPSTH diagonals for the reward and aversive trials. The difference between reward and aversive in the cue and outcome epochs was highly significant for the DANs (Figure 5, red line) but not for the TAN pairs (Figure 5, green line). Thus, the transient changes in noise correlation in the DANs, but not TANs, discriminate between reward and aversive related events.

TANs Show an Unspecific Decrease in Noise Correlation before Cue Ending

Figure 6 presents the analysis of the population JPSTH for the TANs (from 0.5 s before cue onset to 1 s after cue offset and the beginning of the outcome/no-outcome epoch). We grouped the outcome and no-outcome epochs because we did not find significant differences between their JPSTHs (paired t test; p > 0.l6). As was previously shown (Raz et al., 1996; Kimura et al., 2003; Morris et al., 2004), we found that TANs tend to have positive noise correlations. In comparison to the fast increase of the
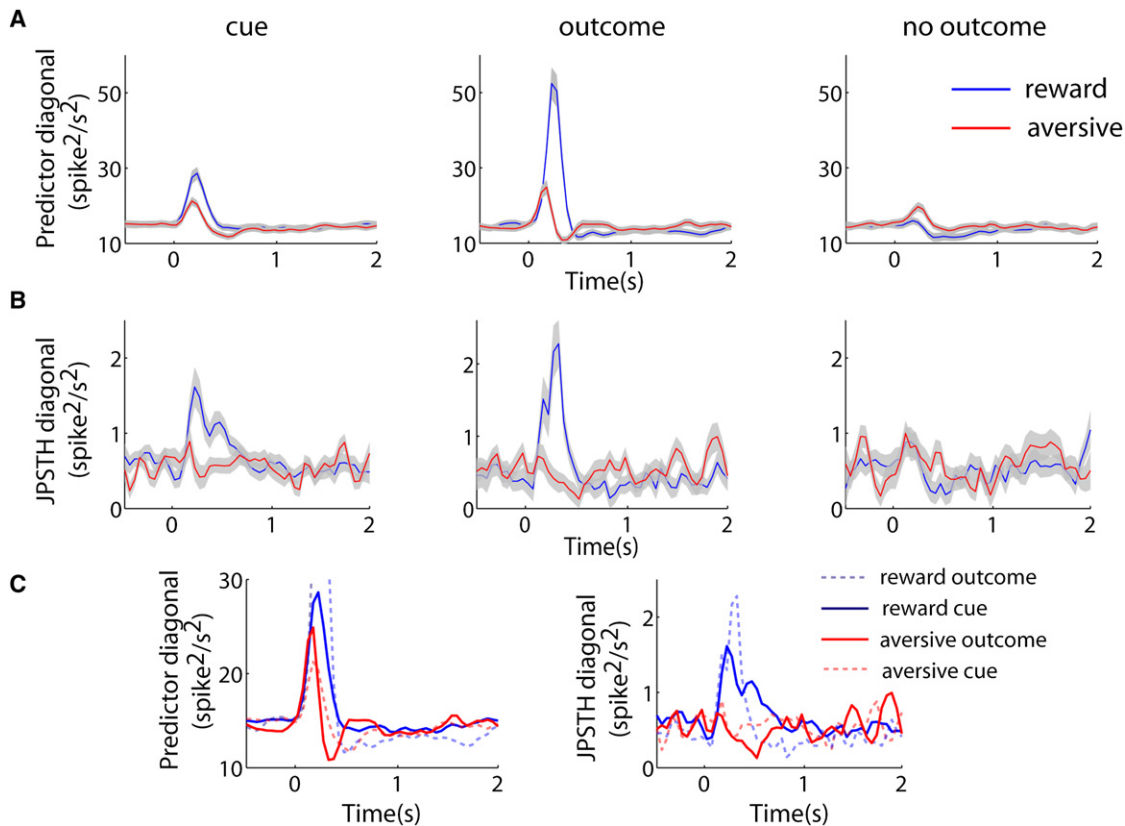
Figure 4. Modulations of DAN Noise Correlation Do Not Mirror Rate Modulation

(A) Common rate modulations: Diagonal of the PSTH predictor (±SEM in gray shading, n = 144 DAN pairs) for the reward (blue) and aversive events (red). Left, cue; middle, outcome; right, no outcome.

(B) Zero lag noise correlation: JPSTH diagonal (±SEM in gray shading) of the DANs for the reward (blue) and aversive (red) events. Same conventions as in (A).

(C) An example of reward and aversive events with similar rate modulation but opposite JPSTH modulations. Left: Predictor diagonal (common rate modulation) for reward cue (blue solid line) and aversive outcome (red solid line). Right : Corresponding JPSTH diagonals (noise correlation modulations). The rate and JPSTH modulation of the other events in (A) and (B) left and middle subplots are given in dashed lines. Although both PSTH predictors (common rate modulations) have a similar positive peak (left), only the diagonal of the JPSTH for the reward cue has positive modulations (right).

noise correlation of the DANs (Figures 3 and 4) following the onset of rewarding cue and outcome, the TAN correlations decreased gradually during the cue epoch and increased in the outcome epoch (Figures 6A and 6B). We found that the TANs correlation and rate modulations tended to be separated in time (Figure 6C).

DISCUSSION

We showed that the responses of cells from the same neuromodulator population (TANs or DANs) tended to have a positive correlation. In comparison to the homogenous responses of the basal ganglia modulators, the neurons of the basal ganglia main axis had diverse responses. Pairs of DANs, as well as pairs of TANs, dynamically modulate their discharge variation (noise correlation) in accordance with events in the behavioral task. The noise correlation between the DANs increased after the cue and outcome events, whereas the TANs noise correlation decreased just before cue offset. Furthermore, although the discharge rate of the DANs increased both in reward and

aversive trials, their noise correlation increased only in the reward trials.

Correlations of the Average Response Set Neuromodulators Apart from the Main Axis

Previous studies have observed that different neuromodulator cells have responses with similar temporal patterns (Graybiel et al., 1994; Schultz, 1998). In this manuscript we quantified the similarity of the temporal pattern of the response (response correlation) and the similarity of the encoding of different events (signal correlation). We showed that in contrast to the basal ganglia neuromodulators, the main axis responses are diverse (Figures 2, S1, and S2). The homogeneous responses of the neuromodulators suggest that these populations as a whole provide the main axis with a scalar message; i.e., the encoding of different DANs, as well as different TANs, is similar. By contrast, the diversity of the main axis responses suggests that its activity is highly independent, which is conducive to a large information capacity (Bar-Gad et al., 2003). The contrast between the diversity of the main axis response and the homogeneity of the
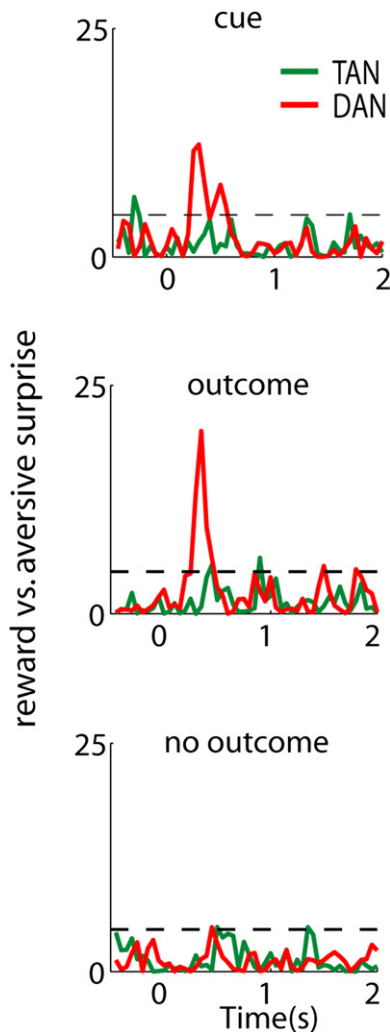
Figure 5. DAN but Not TAN Noise Correlation Differentiates Reward from Aversive Trials
The surprise (−ln(p), p of the paired t test) of the difference between reward and aversive JPSTH diagonals for TANs (green) and DANs (red) neuronal pairs. Dashed line indicates surprise at p = 0.01, values above the dashed line indicate p < 0.01 events. Top, cue; middle, outcome; bottom, no outcome.

modulators was demonstrated in a behavioral task with 18 different events. Nevertheless, we cannot rule out the possibility the recording of neural activity during other tasks or over greater spatial distances (including DANs in the ventral tegmental area and TANs in the caudate or ventral striatum) might reveal other effects. Future studies using a large variety of tasks and wider sampling of basal ganglia neurons should test the consistency and the spatial extent of the homogeneity of the basal ganglia modulators.

Based mainly on the activity of the DANs, it has been suggested that the basal ganglia implements a reinforcement learning algorithm (Schultz et al., 1997). The distinction between the correlation properties of neuromodulators and the main axis is in line with the idea that these populations have a different role in the reinforcement learning system. The neuromodulators'

scalar response is consistent with these neurons being the teacher (e.g., a critic) of this system. The actor, however, requires specificity in encoding of different neuronal elements. Indeed we have found such diversity in the encoding of the main axis neurons.

Limitations of JPSTH Analysis
Several factors limit the interpretation of JPSTH analysis. Variability of latency or excitability effects contribute confounding factors to the JPSTH matrix (Brody, 1999). We could not unequivocally exclude the possibility that these effects contributed to our JPSTHs. For the TANs, however, this is unlikely because the decrease in noise correlation toward the end of the cue epoch does not overlap with the typical fast and transient TAN response (Figure 6C). For the DANs we indeed found a tendency toward coincidence of noise correlation and rate modulations, but the JPSTH analysis dissociated the rewarding and aversive events which nevertheless have similar rate modulations (Figure 4).

Trial-to-trial variability in action might also confound the interpretation of JPSTH analysis (Ben Shaul et al., 2001). Previously we have shown that due to their motor-related sustained responses, the JPSTHs of main axis neuronal pairs are sensitive to false detection of dynamic changes (Arkadir et al., 2002). However, action itself is not encoded in neuromodulators (Kimura et al., 1984; Schultz, 1998; Morris et al., 2004). Hence, we conclude that variability in action did not contribute to the neuromodulator JPSTH analysis.

The neuromodulators' firing pattern is composed of a stereotypic short latency phasic response to external events and tonic Poisson-like activity between these responses. (Kimura et al., 1984; Schultz, 1986; Bayer et al., 2007). This excludes the possibility that opposite signs of neural transients lead to detection of discharge covariation without rate modulations (Friston, 1995). We do not exclude the possibility that the increase in the correlation of the DAN population at the time of the response is due to dynamics of neural transients. Other possibilities are that the increase in correlation is due to changes in the effective connectivity in the dopaminergic neuron network or covariability of inputs. Hence we did not focus on the source of correlation, but refer to the possible effect of the correlation dynamics on the postsynaptic striatal neurons (see below).

Thus the JPSTH analysis of the neuromodulators can be considered valid and provides valuable insights into the encoding of the basal ganglia. Similar studies of the dynamics of noise correlation of the basal ganglia main axis neurons will need to wait for future technical and methodological advances.

Reward-Related Increase in the Noise Correlation of Dopaminergic Neurons
Previous studies have shown that the discharge rate of DANs is modulated by reward, and it was suggested that these neurons encode the reward prediction error (Schultz, 1997; Nakahara et al., 2004; Bayer and Glimcher, 2005; Pan et al., 2005; Morris et al., 2006). Other behavioral factors might also lead to an increase in the dopaminergic rate (Horvitz, 2000; Kakade and Dayan, 2002; Redgrave and Gurney, 2006; Day et al., 2007). We showed that in a classical conditioning task, the activity of
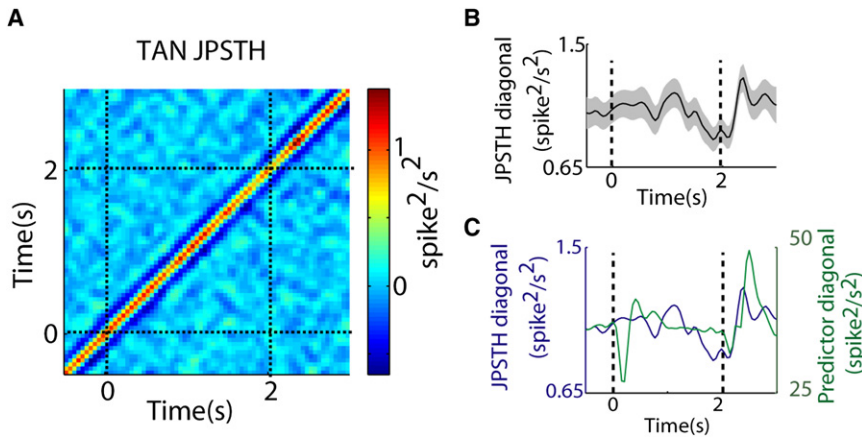
Figure 6. Population JPSTH of TANs Reveals a Decrease in Noise Correlation around Cue Offset

(A) The population JPSTH of the TANs (n = 163 pairs). Bin size 50 × 50 ms, smoothed with a two-dimensional Gaussian filter with SD = 1 bin. Cue appeared at time 0 and lasted until the beginning of the outcome/no-outcome epochs at time = 2 s (marked by dashed lines).

(B) Diagonal of the population JPSTH (smoothed with Gaussian kernel, SD = 1 bin), average in solid line and SEM in light gray.

(C) The mean diagonal of TAN JPSTH (blue) and the mean PSTH predictor (common rate modulation, green) superimposed. The temporal pattern of noise correlation modulations does not reflect the temporal pattern of rate modulations. Specifically, the decrease in noise correlation before the end of the cue epoch is not coincident with rate modulations.

the dopaminergic neurons also increased following nonrewarding events such as the prediction and delivery of airpuffs (Figures 4 and S4, and Joshua et al., 2008). Nonetheless, we found an increase in the noise correlation of DANs to expectation and delivery of reward and not to other events (Figures 3 and 4). These finding for a reward-related increase of the noise correlation extend previous findings of unspecific spike-to-spike (noise) correlations of the DANs (Grace and Bunney, 1983b; Morris et al., 2004).

The modulations of the noise correlation were small compared with the modulations of rate (Figure 4). In a recent study, Schneidman et al. (2006) showed that a weak pairwise correlation might imply a strongly correlated network and provides an effective description of the system. It remains to be determined whether pairwise correlations can yield an effective description of the dopaminergic neurons because current recording methods do not enable in vivo simultaneous recording of many neurons; nevertheless, it demonstrates the potential importance of the current finding of an increase in the pairwise noise correlations.

Dopamine transmission is probably not limited to classical synaptic action because it might also diffuse and reach extrasynaptic receptors (Cragg and Rice, 2004; Arbuthnott and Wickens, 2007; Moss and Bolam, 2008). The spatiotemporal distribution of dopamine effects in the striatum depends on the interaction of release, reuptake, and diffusion. The degree of temporal correlation of the release events influences the relative importance of reuptake versus diffusion. Reuptake by the dopamine transporter is a slow process compared with diffusion of dopamine away from a synapse. Diffusion produces a relatively rapid decrease in concentration if the extracellular concentration of dopamine from other sources is relatively low. However, if dopamine is released from many adjacent sources simultaneously, diffusion is slowed, and reuptake predominates. We used a one-dimensional random walk model to simulate diffusion of dopamine from multiple sources, combined with Michaelis-Menten reuptake kinetics. In Figure S6 we show that the DAN correlation might increase the efficiency of dopamine signaling by reduced clearance through diffusion in the correlated condition. Future studies, using 3D models of the striatum and more comprehen-

sive models of correlated DAN activity, could provide a better understanding of the physiological significance of this phenomenon.

TAN Correlations Are Modulated by Task Timing but Not by Value

Previous studies have shown that TANs are highly synchronized (Raz et al., 1996; Kimura et al., 2003; Morris et al., 2004). However, these studies did not consider the temporal dynamics of the noise correlation. Consistent with these studies, we found that TANs are indeed highly synchronized. Additionally, we found that there is a decrease in their noise correlation just before cue offset (Figure 6). This decrease in noise correlation did not discriminate significantly between the aversive and reward trials (Figures 5 and S5) and appears after the average TAN discharge rate returns to baseline (Figure 6C). It was shown that subpopulations of striatal projection cells encode the outcome stages of the task (Lau and Glimcher, 2007). Thus the decorrelation of TANs at the end of the cue epoch could enable or facilitate this encoding of striatal projection neurons through the cholinergic control of cortico-striatal plasticity (Calabresi et al., 2000; Pisani et al., 2007).

Concluding Remarks

Consistent with the classical concept of dopamine-acetylcholine balance (Barbeau, 1962), the DANs and the TANs have opposing single cell responses. DANs typically increase their discharge rate in response to appetitive predictive cues and outcomes (Schultz, 1998), whereas TANs show a decrease or pause in their background discharge (Aosaki et al., 1994). We found that during the cue epoch the noise correlation of the DANs increases, whereas the correlation for the TANs decreases. We therefore suggest that the concept of dopamine-acetylcholine balance can be extended to the noise correlation of these systems. It is possible that increasing the DAN correlation and the decorrelation of TANs enables an increase and decrease, respectively, in the effective concentrations of striatal dopamine and acetylcholine. The right balance of the basal ganglia neuromodulators and cortico-striatal activity might lead to a maximization of

information in the basal ganglia main axis and an optimal behavioral policy.

EXPERIMENTAL PROCEDURES

All experimental protocols were conducted in accordance with the National Institutes of Health *Guide for the Care and Use of Laboratory Animals* and with the Hebrew University guidelines for the use and care of laboratory animals in research, supervised by the Institutional Animal Care and Use Committee. Behavioral task, data-recoding methods, and single cell analysis appear in detail in previous manuscripts (Joshua et al., 2008, 2009). Here we present a brief summary of these methods and describe methods not used in the previous manuscripts.

Behavioral Task
Two monkeys (L and S, *Macaca fascicularis*, female 4 kg and male 5 kg) were introduced to seven different fractal visual cues, each predicting the outcome in a probabilistic manner (Figure 1A). Fractal cues (full-screen images, 17" LCD monitor, 50 cm in front of the monkey's face) were presented for 2 s. The cues were immediately followed by a result epoch, which could include an outcome (food, airpuff) or no outcome, according to the probabilities associated with the cue. The beginning of the result epoch was signaled by one of three sounds that discriminated the three possible events: a drop of food, an airpuff, or no outcome. Trials were followed by a variable intertrial interval (ITI, monkey S: 3–7 s, monkey L: 4–8 s; Figure 1A).

Recording and Data Acquisition
During the acquisition of the neuronal data, two experimenters (M.J. and A.A.) controlled the vertical position of the eight glass-coated tungsten electrodes (confined with 1.65 mm guide) and real-time spike sorting (AlphaMap, ASD, AlphaOmega). Recorded units were subjected to offline quality analysis that included tests for rate stability, refractory period, waveform isolation, and recording time. First, firing rate as a function of time during the recording session was graphically displayed, and the largest continuous segment of stable data was selected for further analysis. Second, cells in which more than 0.02 of the total ISIs were shorter than 2 ms were excluded from the database. Third, only units with an isolation score (Joshua et al., 2007) above 0.8 (except for the DANs, in which we used a threshold of isolation score > 0.5) were included in the database. The lower threshold used for the DANs is due to the highly dense cellular structure of the SNc, which makes single cell isolation difficult. We also performed the analysis on the high-quality DANs (isolation score > 0.8) and received similar results to those reported. The largest segment for which two simultaneously recorded units fulfilled the inclusion criteria was included in the analysis database only if it was greater than 30 min.

Quantification of Similarity of Temporal Profile of Neuronal Responses: Response Correlation Analysis
For each cell and each behavioral event, we calculated the PSTH. Each of these PSTHs is an n-dimensional vector, where n is the number of 1 ms bins in the histogram (n = 2000 bins, starting at the event onset). This vector was smoothed with a Gaussian window (standard deviation [SD] = 20 ms). To avoid spurious positive correlations due to smoothing of the PSTHs, we padded the PSTH edges with the mirrors of the PSTHs before smoothing. Responses were considered significant if they exceeded the mean of the ITI three times the ITI SD ($3\,\sigma$ rule) for 60 consecutive bins (three times the smoothing SD). To calculate the ITI SD, we randomly pruned the number of ITI trials to the same number of trials for which we calculated the PSTH.

We determined the similarity of the responses of two cells to a behavioral event by calculating the correlation coefficient of the PSTHs. We denoted this correlation the *response correlation*. The response correlation was calculated only for PSTHs with significant responses. To obtain the population response correlation, we grouped all the correlation values, transformed them by a z-transform (Sokal and Rohlf, 1981), and calculated their mean and the standard error of the mean (SEM). The population mean and SEM were obtained by inverse z-transform of these values. For the response

correlation analysis, we used a time window of 2 s starting at the event onset. Because the neuromodulators have a short response, we also performed the analysis on a time window of 1 s, and this analysis gave similar results.

Quantification of Similarity of Responses across Different Events: Signal Correlation Analysis
For each neuron, we computed the PSTHs for all behavioral events (18 events). For this analysis we used the first five 100 ms bins (with no Gaussian smoothing) of the response. We combined all PSTHs into an 18 × 5 matrix, where each row was a task event and each column was a 100 ms bin. For each column, we subtracted that column's mean and then flattened the matrix into a vector of length 90 (18 events × 5 bins). For each pair of simultaneously recorded neurons, we computed the signal correlation by calculating the correlation coefficient of these vectors. For the population average and SEM we z-transformed the correlation coefficients (Sokal and Rohlf, 1981) calculated the average and SEM and obtained the inverse of the transform.

The response and signal correlation were also calculated for pairs of neurons that were not simultaneously recorded and therefore were probably more remote than neurons recorded simultaneously. Analysis of nonsimultaneously recorded cells generated similar trends as the simultaneous ones (i.e., large positive correlations for the neuromodulators versus close to zero average correlations for the main axis); however, correlation values were generally smaller (data not shown).

Quantification of the Temporal Dynamics of the Noise Correlation: JPSTH Analysis
The JPSTH analysis quantifies the temporal dynamics of the modulation of correlations (Gerstein and Perkel, 1969; Aertsen et al., 1989). For this analysis, we calculated the raw JPSTH matrix in which the (t_1,t_2)-th bin was the count of the number of times that a coincidence occurred, in which neuron #1 spiked in time bin t_1 and neuron #2 spiked in time bin t_2 on the same trial (see examples in the first column of Figure S3). To correct for rate modulations we calculated the PSTH predictor (Aertsen et al., 1989). The predictor matrix is the product of the single-neuron PSTHs, i.e., the (t_1,t_2)-th bin is equal to $PSTH_1(t_1)*PSTH_2(t_2)$ (see examples in the second column of Figure S3). The JPSTH was calculated as the subtraction of the number of coincident spikes expected by chance (PSTH predictor) from the raw matrix (see examples in Figure S3). The JPSTH was calculated in bins of 50 ms and smoothed with a two-dimensional Gaussian window with an SD of 50 ms (1 bin).

We also corrected the raw JPSTH using the shift predictor. The different predictors gave the similar results and no trend was found when calculating the difference between these predictors (data not shown). We therefore concluded that the data did not suffer from long-lasting trends because such trends affected the shift predictor and the PSTH predictor differently. We preferred the use of the PSTH correction in the graphical displays in this manuscript because it results in less noisy estimates (Aertsen et al., 1989). In the text, JPSTH refers to the JPSTH corrected by the PSTH predictor.

To group several JPSTHs from several events, we calculated the corrected JPSTH of each event separately and then summed all corrected JPSTHs. For example, the JPSTH for the reward cue is the sum of the corrected JPSTH of the three cues with different probabilities (p = 1/3, 2/3, 1) of receiving reward. We also normalized the JPSTH to obtain correlation coefficient values as introduced by Aertsen et al. (1989); i.e., each bin was divided by the SD of the trial to trial response. Population analysis of the normalized and nonnormalized (but corrected) JPSTH gave similar qualitatively results. In the text, JPSTH refers to the corrected but not normalized JPSTH. To test whether the population JPSTHs for two different events were significantly different, we performed a bin by bin paired t test. The surprise values were obtained by transforming the p value of this test by $-\ln(p)$.

We carried out JPSTH analysis for both the neuromodulators and main axis neurons; however, as we and others have shown, for the neurons of the main axis of the basal ganglia, JPSTH analysis might lead to false detection of correlation dynamics due to variability in the motor-related responses (Arkadir et al., 2002). Indeed many of the JPSTH matrices of the main axis neurons revealed significant marginal effects of the PSTH. This indicates that the PSTH and shift predictors were not able to correct the raw JPSTH reliably, and therefore we excluded the main axis populations from the JPSTH analysis.

REFERENCES

Abeles, M. (1982). Local Cortical Circuits (Berlin, Heidelberg, New York: Springer-Verlag).

Aertsen, A.M., Gerstein, G.L., Habib, M.K., and Palm, G. (1989). Dynamics of neuronal firing correlation: modulation of "effective connectivity". J. Neurophysiol. *61*, 900–917.

Alexander, G.E., DeLong, M.R., and Strick, P.L. (1986). Parallel organization of functionally segregated circuits linking basal ganglia and cortex. Annu. Rev. Neurosci. *9*, 357–381.

Aosaki, T., Tsubokawa, H., Ishida, A., Watanabe, K., Graybiel, A.M., and Kimura, M. (1994). Responses of tonically active neurons in the primate's striatum undergo systematic changes during behavioral sensorimotor conditioning. J. Neurosci. *14*, 3969–3984.

Arbuthnott, G.W., and Wickens, J. (2007). Space, time and dopamine. Trends Neurosci. *30*, 62–69.

Arkadir, D., Ben Shaul, Y., Morris, G., Maraton, S., Goldber, J.A., and Bergman, H. (2002). False detection of dynamic changes. in pallidal neuron interactions by the Joint Peri-Stimulus Histogram method. In The Basal Ganglia VII, L.F.B. Nicholson and R.L.M. Faull, eds. (New York: Kluwer Academic/Plenum Publishers), pp. 181–190.

Averbeck, B.B., and Lee, D. (2004). Coding and transmission of information by neural ensembles. Trends Neurosci. *27*, 225–230.

Averbeck, B.B., Latham, P.E., and Pouget, A. (2006). Neural correlations, population coding and computation. Nat. Rev. Neurosci. *7*, 358–366.

Baker, S.N., Philbin, N., Spinks, R., Pinches, E.M., Wolpert, D.M., MacManus, D.G., Pauluis, Q., and Lemon, R.N. (1999). Multiple single unit recording in the cortex of monkeys using independently moveable microelectrodes. J. Neurosci. Methods *94*, 5–17.

Baker, S.N., Spinks, R., Jackson, A., and Lemon, R.N. (2001). Synchronization in monkey motor cortex during a precision grip task. I. Task-dependent modulation in single-unit synchrony. J. Neurophysiol. *85*, 869–885.

Bar-Gad, I., Ritov, Y., Vaadia, E., and Bergman, H. (2001). Failure in identification of overlapping spikes from multiple neuron activity causes artificial correlations. J. Neurosci. Methods *107*, 1–13.

Bar-Gad, I., Morris, G., and Bergman, H. (2003). Information processing, dimensionality reduction and reinforcement learning in the basal ganglia. Prog. Neurobiol. *71*, 439–473.

Barbeau, A. (1962). The pathogensis of Parkinson's disease: A new hypothesis. Can. Med. Assoc. J. *87*, 802–807.

Bartho, P., Hirase, H., Monconduit, L., Zugaro, M., Harris, K.D., and Buzsaki, G. (2004). Characterization of neocortical principal cells and interneurons by network interactions and extracellular features. J. Neurophysiol. *92*, 600–608.

Bayer, H.M., and Glimcher, P.W. (2005). Midbrain dopamine neurons encode a quantitative reward prediction error signal. Neuron *47*, 129–141.

Bayer, H.M., Lau, B., and Glimcher, P.W. (2007). Statistics of midbrain dopamine neuron spike trains in the awake primate. J. Neurophysiol. *98*, 1428–1439.

Ben Shaul, Y., Bergman, H., Ritov, Y., and Abeles, M. (2001). Trial to trial variability in either stimulus or action causes apparent correlation and synchrony in neuronal activity. J. Neurosci. Methods *111*, 99–110.

Bergman, H., Feingold, A., Nini, A., Raz, A., Slovin, H., Abeles, M., and Vaadia, E. (1998). Physiological aspects of information processing in the basal ganglia of normal and parkinsonian primates. Trends Neurosci. *21*, 32–38.

Brody, C.D. (1999). Correlations without synchrony. Neural Comput. *11*, 1537–1551.

Calabresi, P., Centonze, D., Gubellini, P., Pisani, A., and Bernardi, G. (2000). Acetylcholine-mediated modulation of striatal function. Trends Neurosci. *23*, 120–126.

Centonze, D., Gubellini, P., Pisani, A., Bernardi, G., and Calabresi, P. (2003). Dopamine, acetylcholine and nitric oxide systems interact to induce corticostriatal synaptic plasticity. Rev. Neurosci. *14*, 207–216.

Cragg, S.J., and Rice, M.E. (2004). DAncing past the DAT at a DA synapse. Trends Neurosci. *27*, 270–277.

Day, J.J., Roitman, M.F., Wightman, R.M., and Carelli, R.M. (2007). Associative learning mediates dynamic shifts in dopamine signaling in the nucleus accumbens. Nat. Neurosci. *10*, 1020–1028.

DeLong, M.R. (1971). Activity of pallidal neurons during movement. J. Neurophysiol. *34*, 414–427.

Eggermont, J.J. (1990). The Correlative Brain. Theory and Experiment in Neuronal Interaction (Berlin: Springer-Verlag).

Frank, M.J., Seeberger, L.C., and O'Reilly, R.C. (2004). By carrot or by stick: cognitive reinforcement learning in parkinsonism. Science *306*, 1940–1943.

Friston, K.J. (1995). Neuronal transients. Proc. Biol. Sci. *261*, 401–405.

Fukai, T., and Tanaka, S. (1997). A simple neural network exhibiting selective activation of neuronal ensembles: from winner-take-all to winners-share-all. Neural Comput. *9*, 77–97.

Gawne, T.J., and Richmond, B.J. (1993). How independent are the messages carried by adjacent inferior temporal cortical neurons? J. Neurosci. *13*, 2758–2771.

Gerstein, G.L., and Perkel, D.H. (1969). Simultaneously recorded trains of action potentials: analysis and functional interpretation. Science *164*, 828–830.

Grace, A.A., and Bunney, B.S. (1983a). Intracellular and extracellular electrophysiology of nigral dopaminergic neurons—1. Identification and characterization. Neuroscience *10*, 301–315.

Grace, A.A., and Bunney, B.S. (1983b). Intracellular and extracellular electrophysiology of nigral dopaminergic neurons—3. Evidence for electrotonic coupling. Neuroscience *10*, 333–348.

Graybiel, A.M., Aosaki, T., Flaherty, A.W., and Kimura, M. (1994). The basal ganglia and adaptive motor control. Science *265*, 1826–1831.

Haber, S.N., and Gdowski, M.J. (2004). The basal ganglia. In The Human Nervous System, G. Paxinos and J.K. Mai, eds. (Amsterdam: Elsevier), pp. 676–738.

Horvitz, J.C. (2000). Mesolimbocortical and nigrostriatal dopamine responses to salient non-reward events. Neuroscience *96*, 651–656.

Joshua, M., Elias, S., Levine, O., and Bergman, H. (2007). Quantifying the isolation quality of extracellularly recorded action potentials. J. Neurosci. Methods *163*, 267–282.

Joshua, M., Adler, A., Mitelman, R., Vaadia, E., and Bergman, H. (2008). Midbrain dopaminergic neurons and striatal cholinergic interneurons encode the difference between reward and aversive events at different epochs of probabilistic classical conditioning trials. J. Neurosci. *28*, 11673–11684.

Joshua, M., Adler, A., Rosin, B., Vaadia, E., and Bergman, H. (2009). Encoding of probabilistic rewarding and aversive events by pallidal and nigral neurons. J. Neurophysiol. *101*, 758–772.

Kakade, S., and Dayan, P. (2002). Dopamine: generalization and bonuses. Neural Netw. *15*, 549–559.

Kimura, M., Rajkowski, J., and Evarts, E. (1984). Tonically discharging putamen neurons exhibit set-dependent responses. Proc. Natl. Acad. Sci. USA *81*, 4998–5001.

Kimura, M., Matsumoto, N., Okahashi, K., Ueda, Y., Satoh, T., Minamimoto, T., Sakamoto, M., and Yamada, H. (2003). Goal-directed, serial and synchronous activation of neurons in the primate striatum. Neuroreport *14*, 799–802.

Lau, B., and Glimcher, P.W. (2007). Action and outcome encoding in the primate caudate nucleus. J. Neurosci. *27*, 14502–14514.

Lee, D., Port, N.L., Kruse, W., and Georgopoulos, A.P. (1998). Variability and correlated noise in the discharge of neurons in motor and parietal areas of the primate cortex. J. Neurosci. *18*, 1161–1170.

Lewicki, M.S. (1998). A review of methods for spike sorting: the detection and classification of neural action potentials. Network *9*, R53–R78.

Mink, J.W. (1996). The basal ganglia: focused selection and inhibition of competing motor programs. Prog. Neurobiol. *50*, 381–425.

Morris, G., Arkadir, D., Nevet, A., Vaadia, E., and Bergman, H. (2004). Coincident but distinct messages of midbrain dopamine and striatal tonically active neurons. Neuron *43*, 133–143.

Morris, G., Nevet, A., Arkadir, D., Vaadia, E., and Bergman, H. (2006). Midbrain dopamine neurons encode decisions for future action. Nat. Neurosci. *9*, 1057–1063.

Moss, J., and Bolam, J.P. (2008). A dopaminergic axon lattice in the striatum and its relationship with cortical and thalamic terminals. J. Neurosci. *28*, 11221–11230.

Nakahara, H., Itoh, H., Kawagoe, R., Takikawa, Y., and Hikosaka, O. (2004). Dopamine neurons can represent context-dependent prediction error. Neuron *41*, 269–280.

Nevet, A., Morris, G., Saban, G., Arkadir, D., and Bergman, H. (2007). Lack of spike-count and spike-time correlations in the substantia nigra reticulata despite overlap of neural responses. J. Neurophysiol. *98*, 2232–2243.

Pan, W.X., Schmidt, R., Wickens, J.R., and Hyland, B.I. (2005). Dopamine cells respond to predicted events during classical conditioning: evidence for eligibility traces in the reward-learning network. J. Neurosci. *25*, 6235–6242.

Parent, A., and Hazrati, L.N. (1995). Functional anatomy of the basal ganglia. I. The cortico-basal ganglia-thalamo-cortical loop. Brain Res. Brain Res. Rev. *20*, 91–127.

Percheron, G., and Filion, M. (1991). Parallel processing in the basal ganglia: up to a point. Trends Neurosci. *14*, 55–56.

Percheron, G., Yelnik, J., and Francois, C. (1984). A Golgi analysis of the primate globus pallidus. III. Spatial organization of the striato-pallidal complex. J. Comp. Neurol. *227*, 214–227.

Perkel, D.H., Gerstein, G.L., and Moore, G.P. (1967). Neuronal spike trains and stochastic point processes. II. Simultaneous spike trains. Biophys. J. *7*, 419–440.

Pisani, A., Bernardi, G., Ding, J., and Surmeier, D.J. (2007). Re-emergence of striatal cholinergic interneurons in movement disorders. Trends Neurosci. *30*, 545–553.

Plenz, D. (2003). When inhibition goes incognito: feedback interaction between spiny projection neurons in striatal function. Trends Neurosci. *26*, 436–443.

Raz, A., Feingold, A., Zelanskaya, V., Vaadia, E., and Bergman, H. (1996). Neuronal synchronization of tonically active neurons in the striatum of normal and parkinsonian primates. J. Neurophysiol. *76*, 2083–2088.

Redgrave, P., and Gurney, K. (2006). The short-latency dopamine signal: a role in discovering novel actions? Nat. Rev. Neurosci. *7*, 967–975.

Schneidman, E., Bialek, W., and Berry, M.J. (2003). Synergy, redundancy, and independence in population codes. J. Neurosci. *23*, 11539–11553.

Schneidman, E., Berry, M.J., Segev, R., and Bialek, W. (2006). Weak pairwise correlations imply strongly correlated network states in a neural population. Nature *440*, 1007–1012.

Schultz, W. (1986). Responses of midbrain dopamine neurons to behavioral trigger stimuli in the monkey. J. Neurophysiol. *56*, 1439–1461.

Schultz, W. (1997). Dopamine neurons and their role in reward mechanisms. Curr. Opin. Neurobiol. *7*, 191–197.

Schultz, W. (1998). Predictive reward signal of dopamine neurons. J. Neurophysiol. *80*, 1–27.

Schultz, W., Dayan, P., and Montague, P.R. (1997). A neural substrate of prediction and reward. Science *275*, 1593–1599.

Sokal, R.R., and Rohlf, F.J. (1981). Biometry (New York: W.H. Freeman & Co.).

Tunstall, M.J., Oorschot, D.E., Kean, A., and Wickens, J.R. (2002). Inhibitory interactions between spiny projection neurons in the rat striatum. J. Neurophysiol. *88*, 1263–1269.

Vaadia, E., Haalman, I., Abeles, M., Bergman, H., Prut, Y., Slovin, H., and Aertsen, A. (1995). Dynamics of neuronal interactions in monkey cortex in relation to behavioral events. Nature *373*, 515–518.

Yanai, Y., Adamit, N., Harel, R., Israel, Z., and Prut, Y. (2007). Connected corticospinal sites show enhanced tuning similarity at the onset of voluntary action. J. Neurosci. *27*, 12349–12357.

Zohary, E., Shadlen, M.N., and Newsome, W.T. (1994). Correlated neuronal discharge rate and its implications for psychophysical performance. Nature *370*, 140–143.